Speckle Interferometry Analysis of WDS 18126+3836 (BU 1091) and WDS 18250-0135 (AC 11) Binary Star Systems

Nicholas Bettwy[1], Pat Boyce[2], Mark Harris[2]
[1]Regis High School, New York, NY, US; nicholas.bettwy@gmail.com
[2]Boyce Research Initiatives and Education Foundation (BRIEF), San Diego, CA, US

Abstract

Measurements of mean separation distance and position angle of the binary star systems WDS 18126+3836 (BU 1091) and WDS 18250-0135 (AC 11) were performed using speckle interferometry. The purpose of this study was to determine if the published orbits of these systems may require revision based on our measurements and recent historical data. The observations were made using the Boyce Research Initiative and Education Foundation's 17″ aperture PlaneWave BARO telescope. The measurements yielded a mean separation distance and mean position angle of 0.772″ ± 0.010″ and 316.598° ± 0.755°, respectively, for WDS 18126+3836, and a mean separation distance and mean position angle of 0.916″ ± 0.014″ and 354.43° ± 0.505° for WDS 18250-0135. The measurements for WDS 18126+3836, combined with other recent observations, suggest that the system's orbit may deviate from the previously established ephemeris. Our observations suggest that the currently published orbital solution for WDS 18126+3836 may require reevaluation. The measurements for 18250-0135 closely align with the published orbit, but high inconsistency among historical data limits definitive analysis. Additional observations would benefit evaluation of both systems.

1. Introduction

The orbits of binary star systems are determined by the relative position angle and separation distance between the gravitationally bound stars. The Sixth Catalog of Orbits of Visual Binary Stars, which is maintained by the United States Naval Observatory (USNO), records these measurements based on past observations. Collection and analysis of new measurements allow for more accurate refinement of binary star system orbits.

This work analyzes the position angles and separations of the binary star systems WDS 18126+3836 and WDS 18250-0135. Table 1 below provides specifications for the binary star systems studied in this work, importantly including specifications on orbital grade. Each projected orbit is assigned an orbital grade from 1 to 5; 1 indicates a well-defined orbit, while 5 indicates a poorly constrained orbit. Table 2 details the stellar parameters of each system, and Table 3 details the orbital elements recorded in the 2024 Sixth Catalog of Orbits.

Table 1. Specifications of binary systems considered in this work.

System	Discoverer Number	Orbital Plot References	Grade
WDS 18126+3836	BU 1091	Zirm, H. & Rica, F., 2012	4
WDS 18250-0135	AC 11	Tokovinin, A., 2021	4

Table 2. Stellar parameters of each system.

Note: Primary magnitudes (PMag), secondary magnitudes (SMag), and stellar classes are obtained from the WDS Catalog accessed via Stelle Doppie. Parallax values are obtained from Gaia EDR3 (Gaia Collaboration et al., 2021) where available. For WDS 18250-0135, parallax is obtained from the new Hipparcos reduction (van Leeuwen, 2007), since no Gaia parallax values exist for this system.

System	PMag	SMag	Stellar Class (Primary)	Parallax (mas)	Discovery Date	Number of Observations
WDS 18126+3836	8.66	9.24	F8	6.0480	1888	59
WDS 18250-0135	6.71	7.21	F0	7.49	1854	259

Table 3. Orbital elements of the WDS-published orbits for each system.

System	*P (yrs.)*	*a (")*	*i (°)*	*Ω (°)*	*T_o (yrs.)*	*ω (°)*	*e*
WDS 18126+3836	1297	1.175	138.5	172.9	1933	77.8	0.896
WDS 18250-0135	440.6	0.77	93.3	176.3	1888.7	55.8	0.470

The system WDS 18126+3836 is poorly constrained and classified as grade 4 in the Sixth Catalog of Orbits of Visual Binary Stars. There have been relatively few measurements on this system, with the latest measurement being made in 2016. The system WDS 18250-0135 is also classified as grade 4, and the most recent measurement was made in 2023.

Figures 1a and 1b show the current published orbital plots for each system. The orbital plot for WDS 18126+3836 was last published in 2012 (Zirm, 2012). The orbital plot for WDS 18250-0135 was last published in 2021 (Tokovinin, 2021).

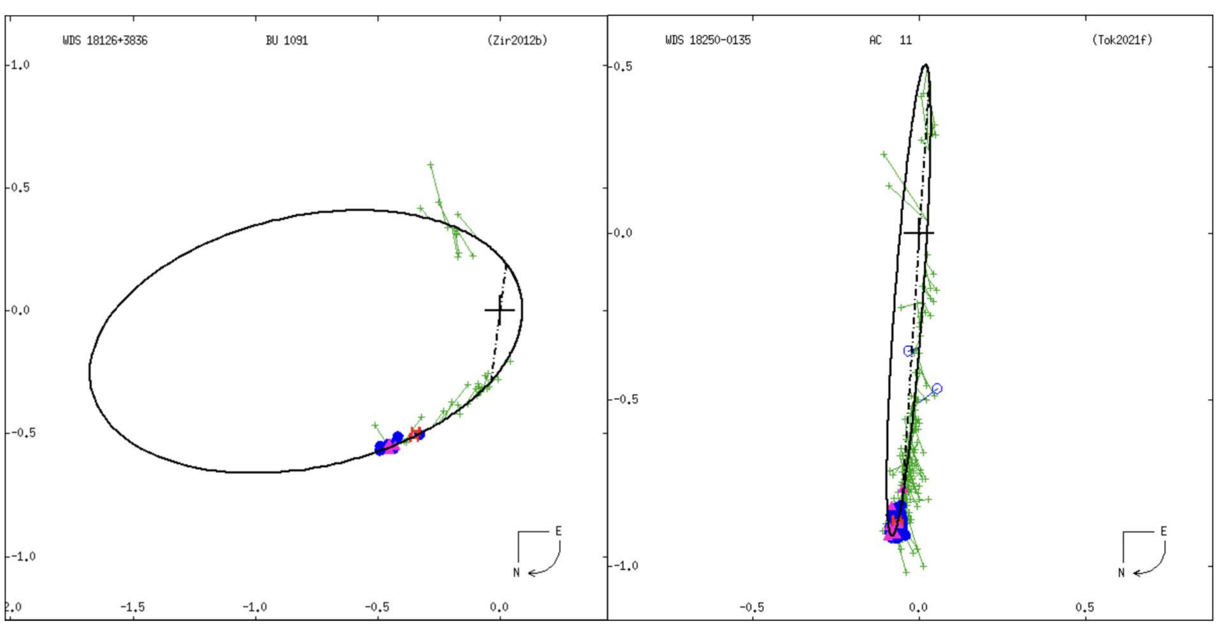

Figure 1a. 6th Orbital Plot for WDS 18126+3836; Figure 1b. 6th Orbital Plot for WDS 18250-0135.

2. Equipment and Methods

Data for this paper was collected using the Boyce Research Initiative and Education Foundation's Boyce-Astro Research Observatory (BARO) located at Tierra Del Sol east of San Diego, CA, equipped with a ZWO 1600 CMOS camera for rapid imaging. The PlaneWave CDK telescope has an aperture of 431 mm and an effective focal length of 7325 mm (2930 mm native; 2.5x Powermate Barlow). This configuration yields a plate scale of 0.106 arcseconds/pixel.

Imaging was taken on June 28th, August 17th, and August 23rd, 2025 through Sloan r filters with an exposure time of 80 milliseconds. The NINA virtual control software was used to direct the telescope's positioning. Calibration images were captured by directing the telescope to the target with a wide field of view and generating images with 60-second exposure times. The Plate Solve 3.80 program used reference stars from the calibration images to determine the relative alignment of the telescope, yielding plate rotation angle and image scale parameters.

Speckle interferometry was used via the Speckle Toolbox software developed by David Rowe as a method of resolving the images by minimizing atmospheric turbulence. Speckle interferometry is effective for analyzing binary stars in such close proximity that variable seeing conditions inhibit image resolution (Beavers et al., 1989). Turbulent airflow and other variable conditions in Earth's atmosphere distort ground-based images of celestial objects, causing them to appear blurred. Speckle Toolbox is used to perform a Fourier mathematical analysis on short exposure images to isolate target star signals from atmospheric disturbance. In this work, large samples (1000 images each) of short exposure (80 milliseconds) images were taken and processed to reduce atmospheric effects and obtain a higher resolution. Speckle Toolbox applied its bi-spectrum phase algorithm to the short exposure images and the data obtained from the calibration image to calculate position angles and separation distances. Figure 2 shows an example of an unresolved image (left) and a resolved image (right) of the primary and secondary star of the binary system WDS 18126+3836 after application of speckle interferometry. The more refined image allows for a more accurate measurement of the stars' relative positions. The statistics detailed in the Results section are based on multiple centroid alignments and data reductions with Speckle Toolbox.

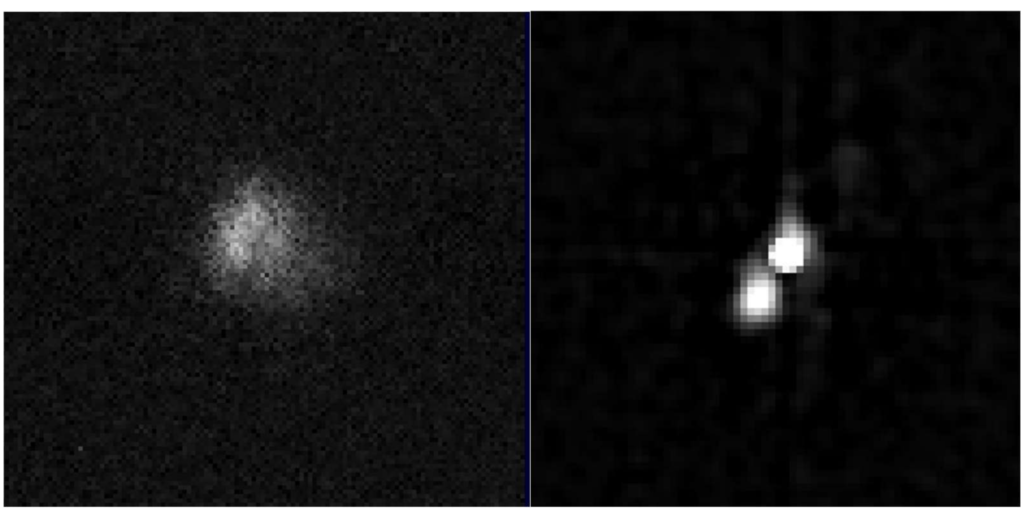

Figure 2. WDS 18126+3836 speckle unresolved (left) and resolved (right). More exact measurements of position angle (θ) and separation (ρ) are obtained after bi-spectrum analysis.

3. Data

The data collected from all systems are specified below in Tables 4 and 5.

Table 4. Data collected for WDS 18126+3836.

WDS 18126+3836		**Discoverer:** BU 1091					
Date	**Epoch**	**Observatory**	**Filter**	**Exposure (msec)**	**Star (S) / Reference (R)**	**Images per cycle**	**Number of cycles**
8/17/25	2025.627	BARO	Sloan r	80	S	1000	1
8/17/25	2025.627	BARO	Sloan r	80	R	300	1
8/23/25	2025.644	BARO	Sloan r	80	S	1000	1
8/23/25	2025.644	BARO	Sloan r	80	R	300	1

Table 5. Data collected for WDS 18250-0135.

WDS 18250-0135		**Discoverer:** AC 11					
Date	**Epoch**	**Observatory**	**Filter**	**Exposure (msec)**	**Star (S) / Reference (R)**	**Images per cycle**	**Number of cycles**
6/28/25	2025.490	BARO	Sloan r	80	S	1000	1
6/28/25	2025.490	BARO	Sloan r	80	R	300	1
8/17/25	2025.627	BARO	Sloan r	80	S	1000	1
8/17/25	2025.627	BARO	Sloan r	80	R	300	1

4. Results

The results of analysis on the data are detailed in Tables 6 and 7 below. Relevant information includes the mean values for position angle (theta) and separation (rho), standard deviation, standard error of the mean, and the projected ephemeris values for theta and rho for the epoch specified. The calculated z-score for each value is also included, indicating how many standard deviations the means are from the ephemeris values; this statistical value is calculated using the formula $Z = \frac{x-\mu}{\sigma}$, with x being the mean measurement value, μ being the ephemeris value, and σ being the standard error of the mean. The reduction results in the following tables are averages from multiple observations to produce more reliable results. The speckle reduction technique described above in the Equipment and Methods section was used to analyze the data.

Table 6. Measured position angle (θ) and separation distance (ρ) for WDS 18126+3836.

WDS 18126+3836

Epoch	Measurement	θ (degrees)	ρ (arcseconds)
2025.6355	Mean	316.598	0.772
	Standard Deviation	0.755	0.010
	Standard Error of the Mean	0.239	0.003
	Ephemeris	316.95	0.807

Theta z-score: $\frac{316.598-316.95}{0.239} \approx -1.47$

Rho z-score: $\frac{0.772-0.807}{0.003} \approx -11.67$

Table 7. Measured position angle (θ) and separation distance (ρ) for WDS 18250-0135.

WDS 18250-0135			
Epoch	Measurement	θ (degrees)	ρ (arcseconds)
2025.5585	Mean	354.43	0.916
	Standard Deviation	0.505	0.014
	Standard Error of the Mean	0.130	0.004
	Ephemeris	354.71	0.911

Theta z-score: $\frac{354.43-354.71}{0.130} \approx -2.15$

Rho z-score: $\frac{0.916-0.911}{0.004} \approx 1.25$

The mean separation distance and separation angle for WDS 18126+3836 are observed to be 0.772″ ± 0.010″ and 316.598° ± 0.755°, respectively. For WDS 18250-0135, the mean separation distance and separation angle are observed to be 0.916″ ± 0.014″ and 354.43° ± 0.505°.

5. Discussion

In Figures 3 and 4, the results from the present work are indicated by the white data points labeled with the technique code *NB* and circled in red.

Figure 3 depicts the historical orbital plot of WDS 18126+3836 from the Sixth Catalog of Visual Binary Star Orbits set against our observed results. This system is categorized as a grade 4 orbit. Our present observation shows a slight deviation from the sixth catalog orbit. The z-score of –11.67 for the separation of this system has a magnitude significantly greater than 3.0, meaning that the new observation differs significantly from the ephemeris prediction relative to the estimated uncertainty. This deviation may suggest the need for reevaluation of this system’s projected orbit. Potential sources of error, such as underestimated uncertainties or measurement bias, could also be involved in this statistic.

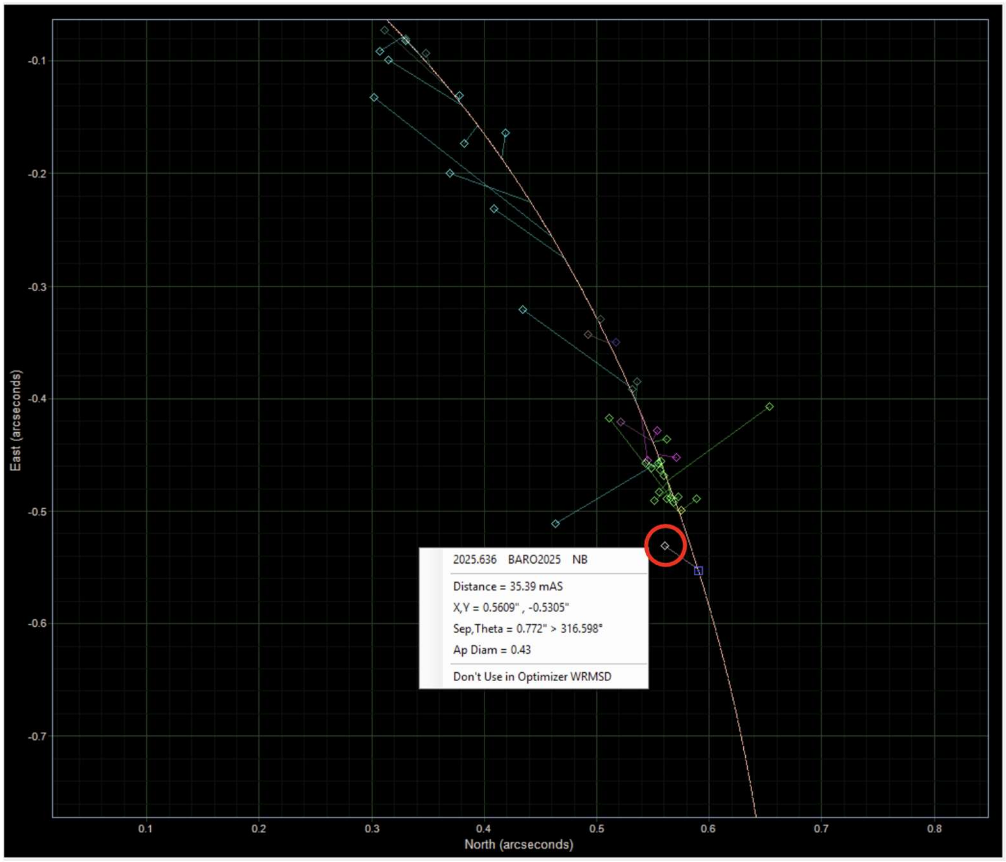

Figure 3. Orbital plot of WDS 18126+3836 with historical data from the Sixth Orbital Catalog.

Figure 4 depicts the historical orbital plot of WDS 18250-0135 set against our observed results. This system is categorized as a grade 4 orbit. Our present observation shows a close alignment with the projected sixth catalog orbit. The observation is 6.5 milliarcseconds (mAS) away from the ephemeris, and z-scores are well below three. However, several inconsistencies and outliers exist in this dataset, making conclusive analysis difficult despite our observation being consistent with the current ephemeris.

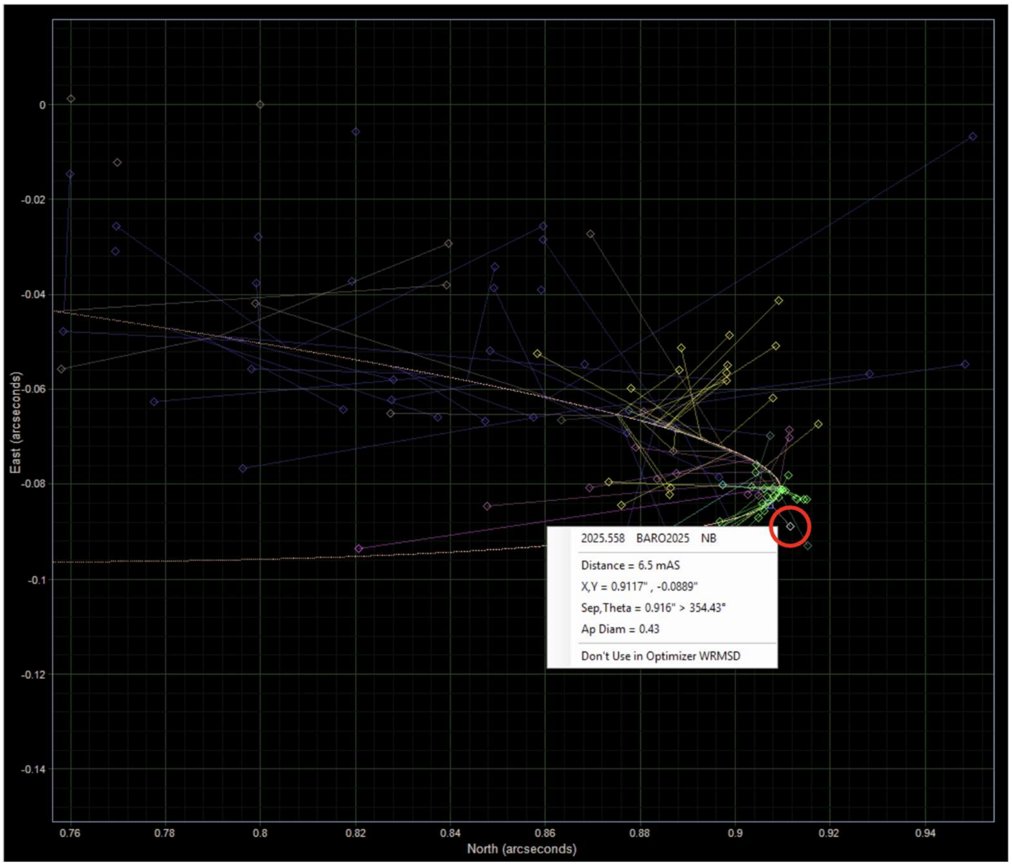

Figure 4. Orbital plot of WDS 18250-0135 with historical data from the Sixth Orbital Catalog.

Comparison between the historical data file for WDS 18126+3836 and the most recent published orbital plot (from 2012) revealed that the ten oldest observations of the system had undergone a quadrant flip input error, in which the position angles had been rotated 180 degrees about the origin. This issue was resolved by manually editing said position angle values in a copy of the historical file. The corrected values aligned with the ten oldest micrometry observations visualized in Figure 1a, which is the most recently published Sixth Orbital Catalog plot.

One observation was identified as an outlier and removed from the dataset for WDS 18126+3836 prior to orbital fitting. Potential outliers were first identified through visual inspection of the orbital plot and then confirmed with three-sigma statistical analysis for both theta and rho values. The residual for each observation was calculated as the observed minus calculated (O-C) difference between the recorded theta or rho value and the corresponding ephemeris value. The mean and standard deviation were then computed across all residuals. The micrometry observation at date 1896.69 yielded a z-score of 4.13 in rho, which exceeded the three sigma threshold for determining outliers, and was thus excluded from the optimization process.

The preliminary optimized orbit for WDS 18126+3836 is shown by the orange ellipse on the plot displayed in Figure 7, which was plotted using the Desmos graphing calculator (Desmos). The updated orbital parameters were produced by using the optimization program in Speckle Toolbox 10.03 (created by David Rowe) to better graphically represent the orbit in accordance with recorded observations of the system. The software uses the optimization technique of "steepest descent with randomization" to achieve an optimization of the fit between the observed data and the calculated orbital model. It does so by iteratively finding the global minimum value for the Weighted Root Mean Square Deviation (WRMSD), avoiding local minima through randomization. WRMSD is a statistic that measures the weighted average deviation between the observed data and the projected orbit, where lower values indicate better agreement between the two. The WRMSD decreased from 57.417 to 34.629 when the new observation was included and the weighting system detailed below was implemented.

Due to the limitations of Speckle Toolbox, weights must be assigned by observation type, not by individual observation, as USNO advises. A python program was created to implement USNO weighting guidance given Speckle Toolbox restrictions by computing composite weights for each individual observation and then averaging over each observation type. The calculation is based on the weighting formula detailed by Hartkopf: *W = W_technique * W_separation * W_n * W_quality* (USNO, 2001). W_technique reflects the intrinsic accuracy of the observation method (e.g. visual micrometry vs. speckle interferometry). W_separation reflects the decline in measurement quality as the observed separation approaches the telescope's specific Rayleigh limit, which is given by the equation $\theta = \frac{1.22\lambda}{D}$, where λ is wavelength and D is aperture. Wavelength information is available directly in the WDS historical data file for each observation. For speckle interferometry observations, the file includes a filter column that records the central wavelength of the filter used, in nanometers, which was used in the Rayleigh limit calculation. For observations with no recorded wavelength in the file, a default wavelength of 550 nm was assumed, corresponding to the center of the visible spectrum. This methodology is consistent with the assumption used by Hartkopf (USNO, 2001). W_n reflects the increased accuracy due to more numerous observations, given by the square root of the number of observations. W_quality halves the weight of observations that have been flagged as uncertain in the WDS historical database. Exact values used to calculate average weights based on observation type are listed in Table 9 (see Appendix A). Access to the code is available through Github (https://github.com/nbettwy/wds-observation-weights-calculation).

Regarding our observation, W_quality was set to 1.0, W_n was set to sqrt(2), W_tech was set to 5.0 based on the BARO telescope aperture, and W_separation was determined based on the measured separation of 0.772″, telescope aperture, and the Sloan r filter used, which corresponds to a wavelength of approximately 625 nm (Fukugita et al., 1996). The calculated relative weight for our new data point resulted in a value of approximately 1.496. The orbital plot of WDS 18126+3836 shown in Figure 5, which weights all included observations with a value of 1.0, yielded a WRMSD of approximately 57.417.

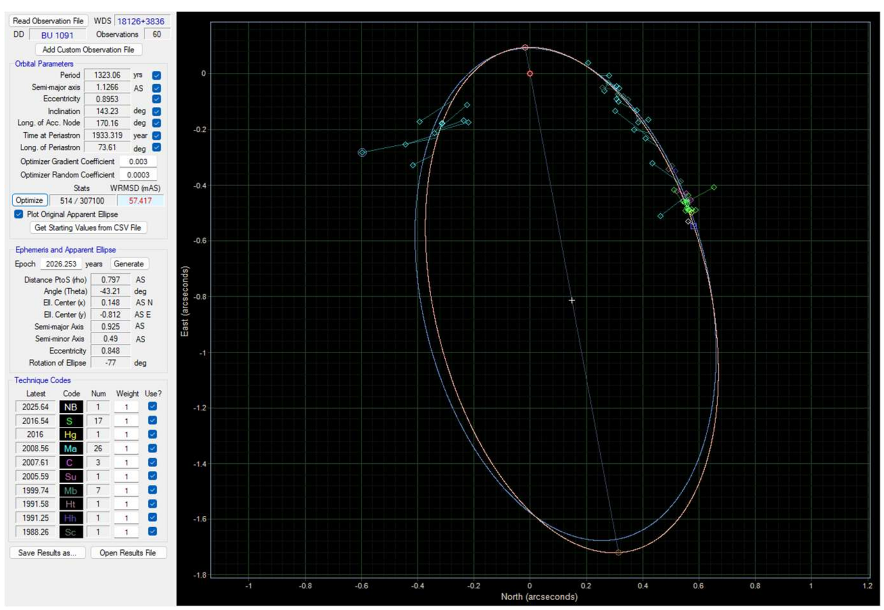

Figure 5. All WDS 18126+3836 observations weighted at 1.0 (WRMSD ~ 57.417).

The orbital plot of WDS 18126+3836 shown in Figure 6, which weights all included observations with relative calculated values, yielded a WRMSD of approximately 34.629. The statistical significance of this decrease in WRMSD from 57.417 to 34.629 should be interpreted cautiously given the nature of the weighting methodology employed. The weights span a large range, and the WRMSD is more strongly influenced by heavily weighted observations. Thus, while a lower WRMSD may suggest a more reliable representation of the system's orbit, it may also reflect the dominance of certain points over others. This is not necessarily a limitation, as the weights are derived from relevant data, meaning higher-weighted points generally reflect more reliable measurements.

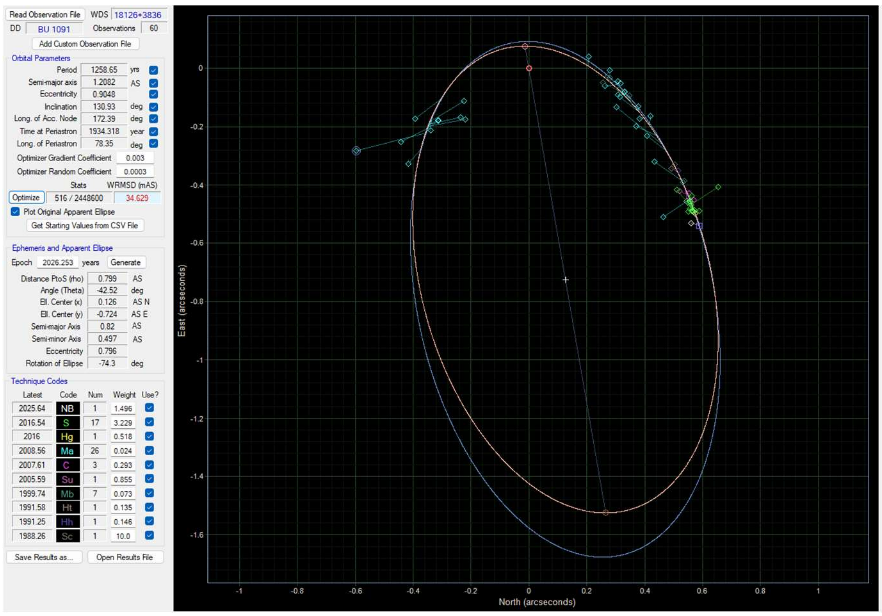

Figure 6. All WDS 18126+3836 observations weighted relatively (WRMSD ~ 34.629).

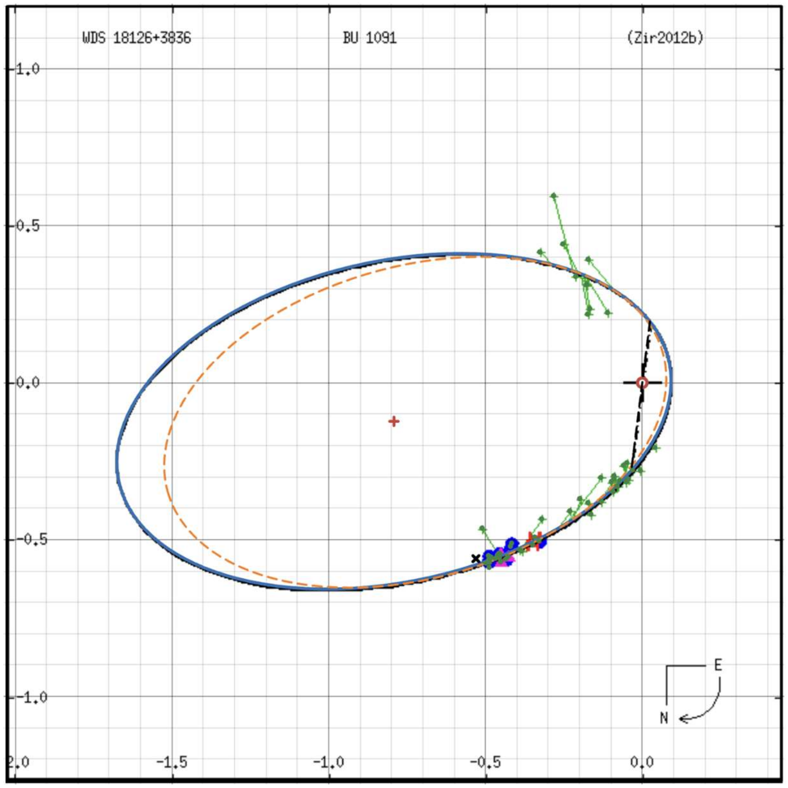

Figure 7. New orbital plot (orange) and old orbital plot (blue) for WDS 18126+3836.

It is important to note that the system's true orbit is its actual orbital path in three-dimensional space. The apparent orbit is a representation of the true orbit projected onto a plane orthogonal to the line of sight of the observer. Seven orbital elements connect the apparent orbit to the true orbit. The orbital elements of WDS 18126+3836 are presented in Table 8 according to the above optimization of the system.

Table 8. Orbital elements before and after orbital optimization for WDS 18126+3836.

Orbital Elements	***P (yrs.)***	***a ('')***	***i (°)***	***Ω (°)***	***T_o (yrs.)***	***ω (°)***	***e***
Historical Data	1297	1.175	138.5	172.9	1933	77.8	0.896
Optimized Data	1258.65	1.2082	130.93	172.39	1934.318	78.35	0.9048

The results show that there are minor changes in the orbit of the system WDS 18126+3836 due to deviation from the published orbit. Direct comparison of the values in Table 8 suggests that this system may be defined by a lower inclination than previously established, with a calculated inclination of 130.93° as opposed to 138.5°. Continued observation of this binary system will likely help refine the orbital elements further.

For the system WDS 18250-0135, the results closely align with the published orbit, as indicated by the low z-scores, however many of the historical speckle observations do not show alignment with the published orbit. The addition of our present observation is not sufficient to improve this system's ephemeris due to the wide degree of inconsistency in the historical data. The widespread misalignment does suggest some level of potential inaccuracy in the current published orbit, however. Continued measurement of this system would greatly benefit analysis of the projected orbit, to a greater degree than WDS 18126+3836.

6. Conclusions

We took measurements of two binary systems, WDS 18126+3836 and WDS 18250-0135, and attempted to determine if the published orbits of these systems may require reevaluation. The results for WDS 18126+3836 appear inconsistent with the WDS-predicted orbit and may indicate the need for a new ephemeris based on updated orbital elements. The results for WDS 18250-0135 appear consistent with the WDS-predicted orbit, however the high level of variability in the historical measurements undermines definitive conclusions about the system. Continued measurement of both systems is encouraged and should help constrain the predicted orbits and orbital elements.

Acknowledgements

This research has made use of the Washington Double Star Catalog maintained by the U.S. Naval Observatory. This research has also made use of data from the European Space Agency (ESA) mission Gaia (https://www.cosmos.esa.int/web/gaia/dpac/consortium). Funding for the DPAC has been provided by national institutions, in particular the institutions participating in the Gaia Multilateral Agreement. In addition, this work utilized David Rowe's Plate Solve 3.80 and Speckle Toolbox 10.03 for data reduction and analysis. Imaging was conducted using Stefan Berg's N.I.N.A. (Nighttime Imaging 'N' Astronomy) software and Nick Hardy's Speckle Interferometry plugin.

We would like to thank Pat Boyce and Grady Boyce from the Boyce Research Initiatives and Education Foundation (BRIEF) for providing guidance and advice throughout the research process. We would like to thank Dr. Rachel Matson for providing the relevant historical data. We also extend gratitude to Dr. Luca Matone from Regis High School for his advice and support.

References

Beavers, W.I., Dudgeon, D.E., Beletic, J.W., Lane, M.T. (1989). Speckle Imaging through the Atmosphere. The Lincoln Laboratory Journal, Volume 2.

BRIEF (2025) Boyce-Astro, www.boyce-astro.org.

Desmos. https://www.desmos.com/calculator.

Fukugita, M., Ichikawa, T., Gunn, J. E., Doi, M., Shimasaku, K., and Schneider, D. P. (1996). The Sloan Digital Sky Survey Photometric System. The Astronomical Journal, 111(4), 1748. https://doi.org/10.1086/117915.

Gaia Collaboration, Brown, A. G. A., Vallenari, A., et al. (2021). Gaia Early Data Release 3: Summary of the Contents and Survey Properties. Astronomy & Astrophysics, 649, A1. https://doi.org/10.1051/0004-6361/202039657.

Genet, R., McCudden, P., and Ellis, M. (2024). Desmos Graphical Analysis of Binary Stars. Journal of Double Star Observations, 20(2), 264.

Harshaw, R., Rowe, D., and Genet, R. (2017). The Speckle Toolbox: A Powerful Data Reduction Tool for CCD Astronomy. Journal of Double Star Observations, 13(1), 52.

Sixth Catalog of Orbits of Visual Binary Stars (WDS-ORB6). 2017. United States Naval Observatory, https://crf.usno.navy.mil/wds-orb6.

Tokovinin, A. (2021). Inf. Circ. IAU (Double Stars), 204.

United States Naval Observatory, Sixth Catalog of Orbits of Visual Binary Stars, adopted from Hartkopf, et al., 2001 AJ 122, 3472, https://crf.usno.navy.mil/wds-orb6.

van Leeuwen, F. (2007). Validation of the New Hipparcos Reduction. Astronomy & Astrophysics, 474(2), 653. https://doi.org/10.1051/0004-6361:20078357.

Washington Double Star Catalog. 2026. United States Naval Observatory, http://www.astro.gsu.edu/wds/.

Zirm, A., and Rica, F. (2012). Inf. Circ. IAU (Double Stars), 176.

Appendix A

Table 9. Relative composite weights and weights averaged for observation type.

Obs. Type	W_tech	W_sep	W_n	W_qual	W	W_avg
	0.1	0.115	√2	1	0.016	
	0.1	0.111	√3	1	0.019	
	0.1	0.156	√2	1	0.022	
	0.1	0.142	1	1	0.014	
	0.1	0.13	√3	1	0.023	
	0.1	0.147	√2	1	0.021	
	0.1	0.126	1	1	0.013	
	0.1	0.116	1	1	0.012	
	0.1	0.217	1	1	0.022	
	0.1	0.091	√3	1	0.016	
	0.1	0.202	√2	1	0.029	
	0.1	0.157	√3	1	0.027	
	0.1	0.162	√2	1	0.023	
	0.1	0.098	√3	1	0.017	
	0.1	0.092	√6	1	0.023	
	0.1	0.098	√3	1	0.017	
	0.1	0.26	2	1	0.052	
	0.1	0.095	√3	1	0.017	
	0.1	0.121	√3	1	0.021	
	0.1	0.228	2	1	0.046	
	0.1	0.182	√3	1	0.032	
	0.1	0.215	√2	1	0.03	
	0.1	0.204	√2	1	0.029	
Ma	0.1	0.234	√2	1	0.033	0.024

	0.1	0.249	1	1	0.025	
	0.1	0.425	1	1	0.042	
	0.1	0.394	√5	1	0.088	
	0.1	0.546	√3	1	0.095	
	0.1	0.516	√2	1	0.073	
	0.1	0.486	√2	1	0.069	
	0.1	0.715	1	1	0.072	
Mb	0.1	0.715	1	1	0.072	0.073
Mc	0.1	0.112	√2	1	0.016	0.016
Sc	10	1	1	1	10	10
Su	5	0.342	1	0.5	0.855	0.855
	5	0.439	1	1	2.197	
	5	0.44	1	1	2.198	
	5	0.442	1	1	2.212	
	7.5	0.681	1	1	5.109	
	7.5	0.681	1	1	5.109	
	5	0.434	1	1	2.17	
	5	0.198	1	1	0.992	
	7.5	0.691	1	1	5.18	
	7.5	1	1	1	7.5	
	5	0.45	1	1	2.25	
	5	0.461	1	1	2.305	
	5	0.464	1	1	2.32	
	5	0.455	1	1	2.277	
	5	0.435	1	1	2.173	
	5	0.143	1	1	0.715	
	7.5	1	1	1	7.5	
S	5	0.538	1	1	2.691	3.229
Hh	1	0.146	1	1	0.146	0.146
Ht	1	0.135	1	1	0.135	0.135
Hg	1	0.518	1	1	0.518	0.518
	1	0.256	1	1	0.256	
	1	0.253	1	1	0.253	
C	1	0.368	1	1	0.368	0.293
NB	5	0.212	√2	1	1.496	1.496